

DESIGN AND STATISTICALLY OPTIMIZE BRIVARACETAM FAST DISSOLVING FILM BY EMPLOYING A 3² FACTORIAL DESIGN

SWETHA M. , JANAKI DEVI SIRISOLLA* 

GITAM School of Pharmacy, GITAM (Deemed to be University), Rushikonda, Visakhapatnam-530045, India

*Corresponding author: Janaki Devi Sirisolla; *Email: jsirisol@gitam.edu

Received: 30 Jan 2026, Revised and Accepted: 01 May 2026

ABSTRACT

Objective: This study aimed to design and statistically optimize Brivaracetam fast dissolving oral film (FDFs) using the solvent casting method by employing a 3²-factorial design.

Methods: The FDFs were made by the solvent casting method, and they were optimized using a 3²-factorial design. The physicochemical properties were evaluated using FTIR, DSC, and SEM. The independent variables in fast-dissolving films were the amount of pectin (A) and PEG400 (B). The dependent variables analyzed were disintegration time (DT) (Y1) and tensile strength (TS) (Y2). The resulting FDFs were characterized for several parameters like drug content, DT, TS, thickness, weight variation, folding endurance, percentage elongation, surface pH and percent drug dissolved in ten minutes (%DD₁₀). The optimized formulation was evaluated for the accelerated stability studies according to ICH guidelines.

Results: FTIR and DSC studies confirm that there was no incompatibility between the drug and excipients. SEM confirms the amorphous nature of the film. The optimised FDF displayed a thickness of 131.27±8.5 µm, a weight variation of 63.8±4.1 mg, a DT of 27±2, a drug content of 97.06±2.4%, a TS of 1.871 N/mm² and a %DD₁₀ of 98.73±2.5%. Accelerated stability studies over three months revealed no significant changes in drug content, mechanical strength, DT and %DD₁₀, confirming the formulation's stability and suitability for therapeutic use.

Conclusion: Brivaracetam FDFs were successfully developed and optimized using a 3² factorial design, exhibiting maximum drug release and minimal DT, demonstrating faster and more effective delivery. Brivaracetam FDFs have great potential as an efficient substitute for conventional oral dosage forms and may significantly boost patient compliance.

Keywords: Folding endurance, Fast dissolving film, Solvent casting, Brivaracetam, Oral dose, Stability

© 2026 The Authors. Published by Innovare Academic Sciences Pvt Ltd. This is an open access article under the CC BY license (<https://creativecommons.org/licenses/by/4.0/>) DOI: <https://dx.doi.org/10.22159/ijap.2026v18i4.58335> Journal homepage: <https://innovareacademic.in/journals/index.php/ijap>

INTRODUCTION

The oral route remains the most preferred method of drug administration due to its convenience, safety, and high patient acceptability. Among emerging oral drug delivery systems, fast dissolving films (FDFs) have gained considerable attention as innovative dosage forms designed to rapidly disintegrate upon contact with saliva in the oral cavity. These thin polymeric films, typically formulated using hydrocolloid-based polymers, dissolve quickly on the tongue or buccal mucosa without the need for water, thereby facilitating rapid drug release and absorption [1, 2]. The rapid disintegration of FDFs enables a faster onset of therapeutic action, improved patient compliance, and enhanced bioavailability compared to conventional oral solid dosage forms [3-5].

Brivaracetam is a third-generation antiepileptic drug approved for the management of focal seizures in patients with epilepsy. Brivaracetam, a biopharmaceutics classification system (BCS) class I drug characterized by high solubility and permeability. Therefore, incorporating brivaracetam into fast dissolving film may provide a convenient and effective alternative dosage form capable of delivering rapid drug release, improved patient adherence, and enhanced therapeutic outcomes without limitations related to solubility or permeability in epilepsy management [7, 8].

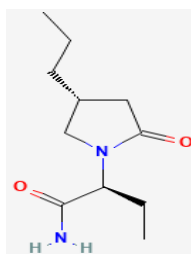


Fig. 1: Structure of brivaracetam

A 3² factorial design was employed to evaluate the effects of two formulation variables at three levels, enabling the assessment of both linear and curvature effects on the response variables. Unlike a 2² design, which captures only linear relationships, the inclusion of three levels allows better optimization of formulation parameters. Box-Behnken design is typically more suitable when three or more independent variables are involved, since the study involved only two independent variables, making the 3² factorial design a more suitable and efficient experimental method [9].

Brivaracetam is an effective antiepileptic drug, but conventional oral dosage forms may show delayed onset of action and swallowing difficulties, particularly in pediatric and geriatric patients. Despite its clinical importance, studies on patient-friendly FDFs for brivaracetam are limited, indicating a clear research gap. Therefore, this study aimed to develop and optimize brivaracetam FDFs using the solvent casting technique, with optimization

via a 3² full factorial design in Design Expert Software Version 12 [10]. The effects of pectin (A) and PEG 400 (B) on DT (Y1) and TS (Y2) were evaluated. This statistical approach provides a novel and systematic optimization strategy, enabling the development of FDFs with rapid disintegration, suitable mechanical properties, and enhanced drug release, offering a promising alternative to conventional brivaracetam dosage forms.

MATERIALS AND METHODS

Materials

Brivaracetam sourced from Dr. Reddy's Laboratories Ltd. (Hyderabad); PEG 400 and pectin from Merck (Mumbai); croscarmellose sodium from Fisher Scientific (Mumbai); citric acid and sucralose from SD Fine-Chem Ltd. (Mumbai). All other chemicals and solvents were analytical or pharmaceutical grade.

Methods

Fast dissolving films were manufactured by the solvent casting method. A clear polymeric solution was obtained by dispersing the required amount of pectin in 10 ml of distilled water and stirring for 30 min. PEG 400 was added to the polymer solution in drops, and the mixture was stirred for another 30 min to ensure complete mixing. Croscarmellose sodium (CCS), citric acid, and sucralose were dispersed in another 10 ml of distilled water in another beaker with continuous stirring for 1 h. Both solutions were subsequently combined to obtain a homogeneous casting solution with a final volume of 20 ml, and brivaracetam was added and mixed. The mixture was then stirred for 2 h at 1000 rpm. The resulting solution was placed under vacuum to eliminate trapped air bubbles and the solution was cast into films on petri plates, dried at 40 °C for 24 h in a hot air oven for the complete evaporation of solvent, the drying process was carried out under ambient laboratory humidity conditions (approximately 50–60% relative humidity, and the oven airflow was maintained at a constant setting to provide uniform heat distribution during drying. Then the dried film was cut to desired sizes (2×2 cm²), with each film containing 25 mg of brivaracetam, corresponding to a single dose and stored in airtight containers for evaluation [11, 12].

Table 1: Formulae of brivaracetam FDFs

Formulation	Coded level A	Coded level B	Pectin (mg)	PEG 400 (ml)	Brivaracetam (mg)	CCS (mg)	Citric acid (mg)	Sucralose (mg)	Water (ml)
F1	-1	1	400	0.6	25	0.1	10	10	20
F2	-1	0	400	0.5	25	0.1	10	10	20
F3	-1	-1	400	0.4	25	0.1	10	10	20
F4	0	-1	500	0.4	25	0.1	10	10	20
F5	0	0	500	0.5	25	0.1	10	10	20
F6	0	1	500	0.6	25	0.1	10	10	20
F7	1	-1	600	0.4	25	0.1	10	10	20
F8	1	0	600	0.5	25	0.1	10	10	20
F9	1	1	600	0.6	25	0.1	10	10	20
VO*	-	-	563.56	0.4	25	0.1	10	10	20

Coded levels -1, 0, and +1 represent low, medium, and high concentrations of each factor, VO-validated optimized (checkpoint formulation)

3² Factorial design

A 3² full factorial design was employed to investigate the influence of two independent variables at three levels on the formulation characteristics of the fast dissolving films. The design generated nine experimental formulations, representing all possible combinations of the selected factor levels. The experimental layout of these formulations is presented in table 1. In addition, checkpoint formulation (VO) was prepared to validate the predictive accuracy of the developed model. Factorial design (two factors, three levels) was employed with Design-Expert® software (Version 12.0.0, Stat-Ease Inc., Minneapolis, USA) used to examine the effect of pectin (A) and PEG 400 (B) on DT (Y1), and TS (Y2) [13]. Table 2 details the design matrix and response variables studied. ANOVA evaluated the significance of regression coefficients and their effects on responses, using p-values and F-values.

Table 2: The variables with their levels in a 3²-factorial design for the development of brivaracetam FDFs

Levels	Pectin (mg) (A)	PEG 400 ml (B)
-1 (Low)	400	0.4
0 (Medium)	500	0.5
1 (High)	600	0.6

*Coded levels -1, 0, and +1 represent low, medium, and high concentrations of each factor, selected from preliminary studies.

FDFs characterization

FTIR investigations

To analyze a sample, it was mixed with potassium bromide and made into pellets, which were used under high pressure. These pellets were scanned over a specific wavelength range, 4000 to 400 cm⁻¹, and the resulting spectra were compared to the standard frequencies of brivaracetam. FTIR graphs were generated for both the pure drug and optimized formulation. (Manufacturer: Bruker Optics GmbH Ettlingen, Germany, model; Vertex 70 FTIR Spectrometer [14].

DSC

Samples (2–5 mg) were sealed in aluminium pans and scanned from 30 to 300 °C at 10 °C/min under nitrogen flow [15]. DSC generated thermograms of the materials. Thermal data were acquired with a TA-501 PC DSC (Shimadzu Corporation, Kyoto, Japan).

SEM

SEM examined film morphology. Samples were mounted on metal stubs with double-sided tape and gold-coated at 10 mA for 20 s. Images were captured at 2.00 KX magnification operated at an accelerating voltage of 10 kV (EVO series, Carl Zeiss AG, Oberkochen, Germany) [16].

Evaluation of brivaracetam FDFs

Weight variation

Three films (2×2 cm²) with each unit representing a single-dose film containing 25 mg brivaracetam were randomly chosen, individually weighed, and compared to their average weight to assess weight variation. Weight variation was determined by individually weighing several film units of the same dimensions to assess the uniformity of the film mass, which corresponds to dose uniformity due to the homogeneous distribution of the drug within the film matrix [17].

Film thickness

Film thickness was measured with a micrometre screw gauge at multiple points; the average determined uniformity [18].

Folding endurance

Films (2×2 cm², n=3 per formulation) were cut with a sharp blade. A strip from each was repeatedly folded at one spot until breakage; the number of folds endured gave the value. Means were calculated from three replicates [19]. Folding endurance ranged from 100–140, indicating low film brittleness.

TS

TS represents the maximum stress a film strip withstands before breaking, calculated via a standard formula.

$$\text{Tensile strength} = \frac{\text{Load at failure (N)}}{\text{Strip thickness (mm)}} \times \text{strip width (mm)}$$

Percentage elongation

Percent elongation measured changes from initial to extended film length using a 50 kg load cell on an Instron tester. Samples (2×2 cm²) were clamped vertically; the lower clamp pulled at 100 mm/min while the upper held firm. Value were computed with the standard equation [20]

$$\% \text{ elongation} = \frac{\text{Increase in length of strip}}{\text{Initial length of strip}} \times 100$$

Surface pH

Surface pH tested potential *in vivo* irritation, as acidic or alkaline values could irritate the oral mucosa. Films were placed in test tubes, wetted with 1.0 ml distilled water for 30 s, to allow hydration of the film surface. After allowing the film to equilibrate for approximately 1 min, the electrode of a calibrated digital pH meter was gently placed in direct contact with the wetted film surface, and the pH value was recorded once the reading became stable [21].

DT

In vitro DT was determined visually in a petri dish containing 20 ml of simulated salivary fluid pH 6.8, according to the general principles described in USP<701>-disintegration test. Each 2×2 cm² film was placed in a Petri dish maintained at 37±0.5 °C. The time required for the film to completely disintegrate without leaving any visible residue was recorded using a stopwatch [22].

Drug content

Three films (2×2 cm²) were dissolved in 100 ml of pH 6.8 simulated salivary fluid for 30 min. Aliquots (1 ml, diluted to 10 ml) were measured at 210.0 nm via a UV spectrophotometer.

In vitro dissolution study

Dissolution profiles were run on USP Type II (paddle) apparatus (DS 8000, Labindia Analytical Instruments Pvt. Ltd., Mumbai, India) using 300 ml the use of larger dissolution medium ensures sink condition, uniform hydrodynamic conditions, and reproducible drug release profiles for thin film formulations pH 6.8 simulated salivary fluid at 37±0.5 °C, stirred at 50 rpm to ensure uniform hydrodynamic conditions and reproducible drug release without causing excessive turbulence. Samples were withdrawn every 30-second intervals during the initial study to determine the rapid drug release behavior of the fast dissolving films. At each time point, an equal volume was replaced with fresh medium to maintain the sink conditions, and absorbance was measured at 210.0 nm spectrophotometrically [23, 24].

Stability studies

The stability of the optimized fast dissolving film formulation was evaluated according to the guidelines described in ICH Q1A(R2) for stability testing of pharmaceutical products. Stability testing was evaluated for the optimized F2 formulation over 3 mo. Packs sealed in aluminum foil were stored at 40±2 °C and 75±5% relative humidity. Samples were withdrawn at predetermined intervals (0, 1, 2, and 3 mo) and assessed for drug content, *in vitro* release, DT, and TS [25]. To statistically confirm the stability of the optimized formulation, a paired Student's t-test was performed comparing the initial and three mo values for key parameters [26].

RESULTS AND DISCUSSION

FTIR

Fig. 2a show a broad peak at 3360 cm⁻¹ for –OH stretching (hydroxyl groups), 2850 cm⁻¹ for –CH stretching (aliphatic chains), 1680 cm⁻¹ for C=O stretching (carbonyl), 1421 cm⁻¹ for C–N stretching (amine), 1120 cm⁻¹ for C–O stretching (oxygen functions), and 960 cm⁻¹ for =C–H bending (aromatic substitution). The excipients, including PEG, pectin, CCS, citric acid, and sucrose, displayed their characteristic peaks, such as 3450 cm⁻¹ for PEG (O–H stretching), 1734 cm⁻¹ ester carbonyl (C=O) stretching, 1570 cm⁻¹ for CCS (COO⁻ asymmetric stretching), 2900 cm⁻¹ for sucrose (C–H stretching) characteristic peaks were also present in the spectra of the optimized fast dissolving film (fig. 3), with only minor peak broadening

observed due to the polymer matrix. Importantly, no significant peak shifts or disappearance of characteristic peaks were identified. Overall, the FTIR analysis confirms that there are no significant chemical interactions, ensuring the stability and compatibility of the brivaracetam and the selected excipients.

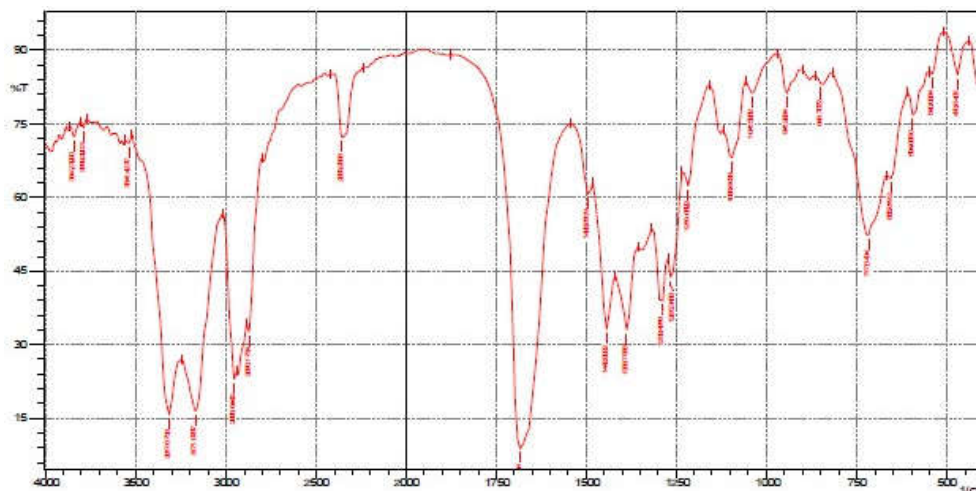


Fig. 2: FTIR of pure brivaracetam showing the characteristic functional group vibrations, the x-axis represents wavenumber (cm^{-1}) and the y-axis represents percentage transmittance (%T)

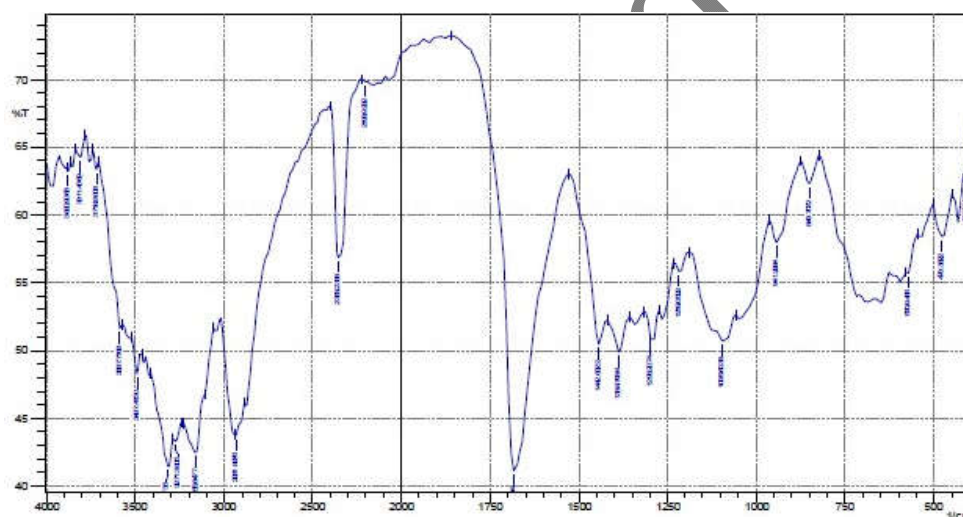


Fig. 3: FTIR of optimized FDF, the x-axis represents wavenumber (cm^{-1}), and the y-axis represents percentage transmittance (%T). The retention of the characteristic peaks without significant shifts indicates compatibility between brivaracetam and the excipients used in FDFs

DSC

The DSC analysis of pure brivaracetam (fig. 4) revealed an initial endothermic peak at $81.91\text{ }^{\circ}\text{C}$ (onset: $79.49\text{ }^{\circ}\text{C}$; endset: $80.39\text{ }^{\circ}\text{C}$) with an enthalpy change of -52.08 J/g . A second, sharp endothermic peak appeared at $232.23\text{ }^{\circ}\text{C}$ (onset: $224.07\text{ }^{\circ}\text{C}$; endset: $238.00\text{ }^{\circ}\text{C}$) with an enthalpy of -34.92 J/g , corresponding to the melting point (T_m) of brivaracetam. The sharpness and intensity of this peak indicate the high crystalline nature and purity of the drug. A broad endothermic peak was observed at $62.81\text{ }^{\circ}\text{C}$ (onset: $43.30\text{ }^{\circ}\text{C}$; endset: $108.86\text{ }^{\circ}\text{C}$) with a high enthalpy value (-354.39 J/g). This was due to the evaporation of bound moisture and plasticiser-associated water within the polymeric matrix. The DSC thermogram of the optimized brivaracetam fast-dissolving film exhibits multiple thermal events. Characteristic endothermic melting peak of brivaracetam is slightly shifted from peaks around $225.20\text{ }^{\circ}\text{C}$, $236.03\text{ }^{\circ}\text{C}$, and $243.24\text{ }^{\circ}\text{C}$. The reduced intensity and broadening of these peaks indicate a decrease in crystallinity and partial amorphisation of the drug within the film matrix, shown in fig. 5. An endothermic peak was observed around $70\text{--}90\text{ }^{\circ}\text{C}$ due to the loss of absorbed moisture, indicating the molecular dispersion of the drug within the polymer matrix. The absence of any additional unexpected peaks or exothermic transitions in the film thermogram indicates that no chemical interaction occurred between brivaracetam and the excipients. These results indicated that brivaracetam was successfully incorporated into the polymer matrix and may exist in a partially amorphous state, which helps in enhanced dissolution of the FDFs.

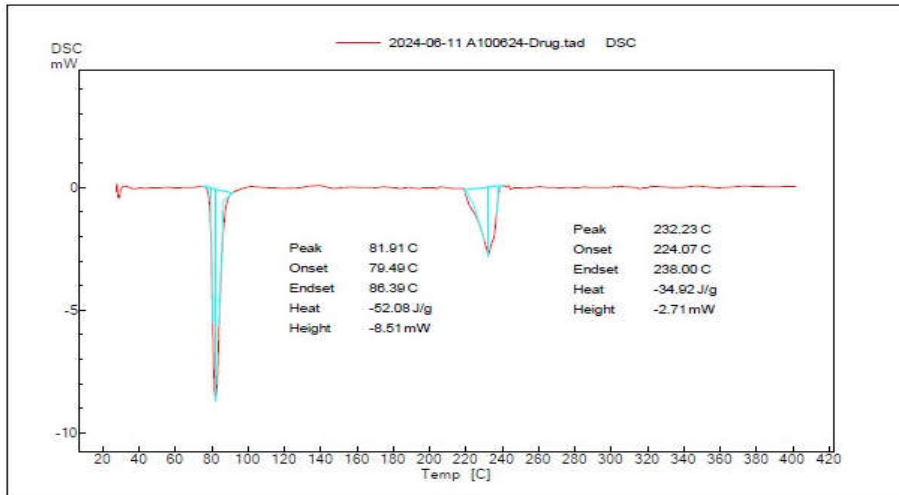


Fig. 4: DSC of pure brivaracetam showing a characteristic sharp melting endothermic peak at approximately 232 °C, confirming the crystalline nature of the drug. The x-axis represents temperature (°C) and the y-axis represents heat flow (mW)

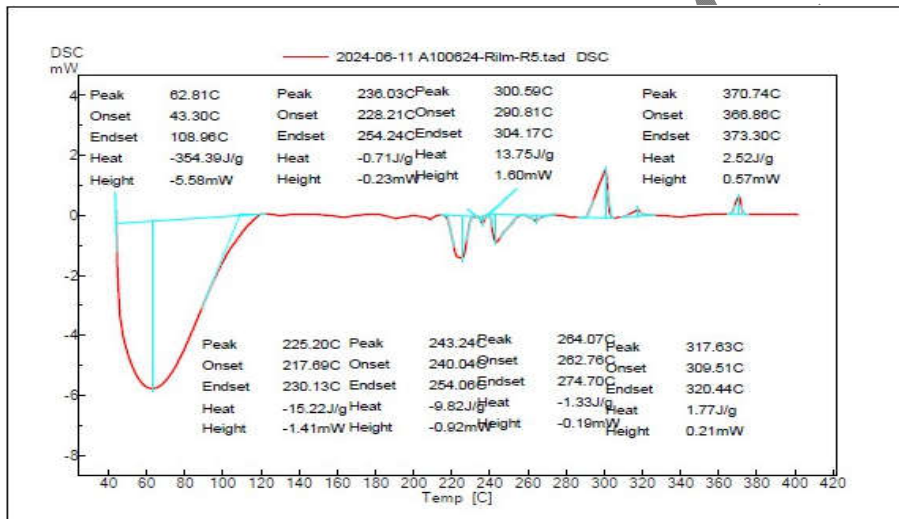


Fig. 5: DSC of optimized FDF, the thermogram shows multiple thermal events associated with the polymer matrix, while the characteristic melting peak of brivaracetam (232 °C) is absent or reduced, indicating molecular dispersion of the drug within the film matrix. The x-axis represents temperature (°C) and the y-axis represents heat flow (mW)

SEM

SEM analysis (fig. 6) revealed that the pure brivaracetam exhibits well-defined, plate-like crystalline particles with smooth surfaces and sharp edges, confirming its crystalline nature, which is consistent with DSC findings. Whereas optimized FDFs of SEM show an amorphous nature, as shown in fig. 7.

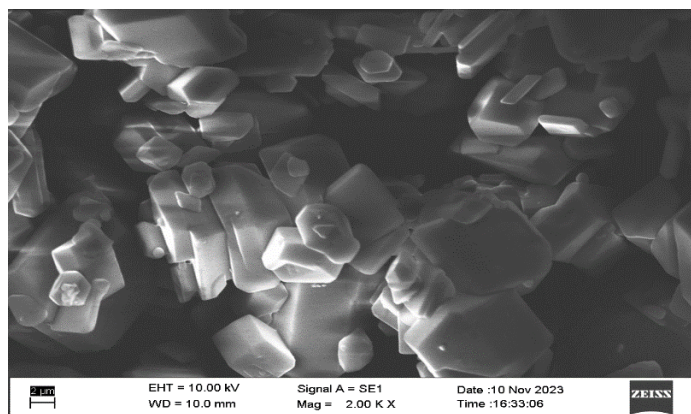


Fig. 6: SEM image of pure brivaracetam with a magnification of 2.00 KX and 10 kV accelerating voltage

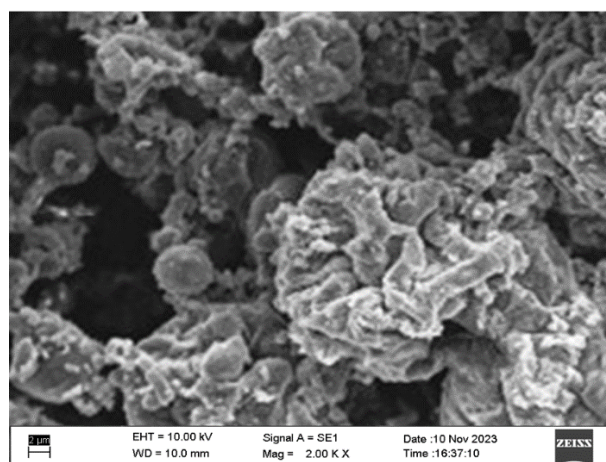


Fig. 7: SEM image of brivaracetam FDFs with a magnification of 2.00 KX and 10 kV accelerating voltage

Evaluation of oral thin films

The developed films were assessed for a variety of characteristics, including physicochemical and morphological characteristics. Every film that formed was transparent and had a uniform thickness. The films were sufficiently elegant to be seen, and their surfaces were smooth, as shown in table 3.

Table 3: Physical appearance and film-forming characteristics of brivaracetam FDFs

Batch	Visual appearance	Surface	Film-forming capacity
F1	Transparent	Smooth	Good
F2	Transparent	Smooth	Good
F3	Transparent	Smooth	Good
F4	Transparent	Smooth	Good
F5	Transparent	Smooth	Good
F6	Transparent	Smooth	Good
F7	Transparent	Smooth	Good
F8	Transparent	Smooth	Good
F9	Transparent	Smooth	Good

Independent film samples (n=6)

Thickness

Film thickness governs the diffusion path length and hydration rate, thereby directly controlling disintegration and drug release kinetics in FDFs. Increased thickness enhances mechanical strength and drug loading, but reduces wetting efficiency and slows drug dissolution. FDF thickness was measured via screw gauge. Table 4 lists values for all formulations (131.7±8.5 to 175.2±8.6 μm). Higher pectin content markedly increased film thickness; combining elevated pectin with PEG 400 yielded thicker, more uniform films.

Table 4: Physical and mechanical properties of brivaracetam FDFs

Batch	Thickness (μm)	Weight variation (mg)	Folding endurance	% Elongation
F1	132.2 \pm 10.1	36.1 \pm 5.1	101.67 \pm 8.9	3.01 \pm 0.6
F2	131.7 \pm 8.5	33.8 \pm 4.1	109.33 \pm 7.5	3.18 \pm 0.7
F3	138.5 \pm 9.1	34.5 \pm 3.5	119.01 \pm 6.4	3.29 \pm 0.6
F4	151.2 \pm 10.3	32.5 \pm 2.2	122.36 \pm 6.6	3.38 \pm 0.5
F5	168.2 \pm 8.7	34.9 \pm 3.5	128.67 \pm 5.9	3.6 \pm 0.4
F6	154.8 \pm 6.8	33.7 \pm 1.5	130.67 \pm 5.7	3.5 \pm 0.7
F7	168.9 \pm 9.9	35.7 \pm 2.4	134.33 \pm 5.3	3.76 \pm 0.5
F8	173.2 \pm 9.4	35.9 \pm 6.2	137.65 \pm 7.1	3.56 \pm 0.7
F9	175.2 \pm 8.6	36.1 \pm 5.1	137.33 \pm 8.4	3.44 \pm 0.8
VO	135.6 \pm 7.3	34.9 \pm 6.2	112.32 \pm 7.3	3.26 \pm 0.5

*n=6 independent film samples, mean \pm SD

Weight variation

Weight variation in FDFs is primarily governed by non-uniform film thickness and solvent evaporation during casting, resulting in differences in mass per unit area. As the drug is uniformly distributed within the matrix, these variations lead to proportional fluctuations in drug content and dose uniformity. The produced films' weights ranged from 33.8 \pm 4.1 to 36.1 \pm 5.1 mg, suggesting consistent film production across batches. Pectin (A) and PEG 400 (B) concentrations had the most significant effects on variations in film weight. The low standard deviation readings indicate the prepared films' consistent weight. Table 4 displays results.

Folding endurance

Folding endurance gauges film brittleness. Results showed it increased with polymer and plasticizer levels. Table 4 reports values from 101.67 \pm 8.9 to 137.33 \pm 8.4 across FDFs, confirming sufficient mechanical strength. F2 was selected as optimized formula for its balanced profile, prioritising overall performance over maximum numeric folding endurance. These formulations folding endurance in line with the formulations prepared by Costa BS *et al.*, 2025, these formulations having a folding endurance range from 176 \pm 3.76 to 213 \pm 2.30 [27].

The percentage of elongation

Percentage elongation reflects the extent of polymer mobility and flexibility under tensile stress. Higher elongation indicates greater plasticity and reduced brittleness, contributing to improved mechanical integrity of the film. Table 4 displays the % elongation of all formulations of FDFs. The polymer's elasticity and plasticity are revealed by the percentage elongation study, and the films' results ranged from 3.01 \pm 0.6 to 3.76 \pm 0.5%. Formulation F2 (3.18) was chosen as the optimal batch because of its balanced flexibility, lower polymer load, and appropriateness for FDF applications. The data showed that greater polymer concentrations led to increased percentage elongation.

Surface pH

All FDFs exhibited a surface pH of 5.83 \pm 0.35–6.66 \pm 0.26 (table 5), close to the physiological pH of saliva. This minimises the risk of sublingual irritation, enhancing patient tolerability. These formulations surface pH in line with the formulations prepared by Mitra *et al.*, 2026, these formulations having a surface pH range from 6.4 \pm 0.3 to 6.7 \pm 0.2 [28].

Table 5: Physicochemical and mechanical evaluation of brivaracetam FDFs

Batch	DT (sec)	Surface pH	Drug content (%)	TS(N/mm ²)
F1	28 \pm 1	5.93 \pm 0.20	94.45 \pm 1.3	1.99 \pm 0.09
F2	27 \pm 2	6.44 \pm 0.63	97.06 \pm 2.4	1.78 \pm 0.12
F3	30 \pm 2	6.51 \pm 0.51	94.6 \pm 1.9	1.85 \pm 0.16
F4	34 \pm 2	5.83 \pm 0.35	93.09 \pm 1.2	2.19 \pm 0.25
F5	35 \pm 2	6.66 \pm 0.26	92.21 \pm 1.4	2.15 \pm 0.31
F6	38 \pm 1	6.59 \pm 0.31	95.48 \pm 1.5	2.26 \pm 0.26
F7	41 \pm 2	6.23 \pm 0.51	94.05 \pm 1.6	2.34 \pm 0.17
F8	47 \pm 1	6.31 \pm 0.21	95.28 \pm 1.7	2.47 \pm 0.24
F9	44 \pm 2	6.45 \pm 0.35	95.75 \pm 1.4	2.57 \pm 0.22
VO	30 \pm 1	6.51 \pm 0.27	98.76 \pm 1.5	2.30 \pm 0.12

*n=6 independent film samples, mean \pm SD

Drug content

Formulated films showed drug content of 93.09 \pm 1.2% to 97.06 \pm 2.4%, meeting IP limits (85–110%; table 5). Consistent values across films confirmed excellent content uniformity.

DT

Disintegration time (DT) assessed via the DT test apparatus revealed that polymer concentration prolonged DT. All FDFs disintegrated in 27 \pm 2 to 47 \pm 1s (table 5), confirming rapid breakdown. PEG 400 enhances the hydration of the film by improving water penetration into the polymer network. This increased wettability facilitates faster swelling and erosion of the film matrix, thereby reducing the DT of the FDFs. Films containing lower polymer concentrations exhibited faster disintegration, whereas higher polymer levels resulted in increased disintegration time due to the formation of a denser polymeric matrix. Similarly, higher plasticizer levels tended to slightly increase disintegration time by enhancing film integrity [26]. Optimized F2 achieved the fastest DT (27 \pm 2 seconds) due to an ideal polymer-plasticizer balance. These formulations show the least DT compared to formulations prepared by Costa BS *et al.*, 2025, these formulations having a DT of 1.12 \pm 0.03 min [29].

TS

The produced films' TS ranged from 1.78 ± 0.12 to 2.57 ± 0.22 N/mm², suggesting that all formulations had sufficient mechanical strength. The solvent system that had to be cast had a higher viscosity. It influences the film's brittleness and thickness. PEG 400 decreases the rigidity of the polymer matrix by acting as a plasticizing agent. As the concentration of PEG 400 increases, the polymer chains become more flexible, which may lead to a slight reduction in TS but improves the overall flexibility and folding endurance of the film [24]. The results, which are displayed in table 5, demonstrated that the TS of FDFs increases as the concentration of polymer increases. These formulations show better TS compared to the formulation prepared by Godge RK *et al.*, 2025, which had a TS of 2.87 N/mm² [30].

In vitro drug release

In vitro release profiles (n=6, mean±SD) for all formulations (F1-F9) appear in Figs. 8–10, demonstrated a rapid drug release, nearly $93.85 \pm 3.7\%$ to $98.94 \pm 4.6\%$ within 10 min. The enhanced drug release may be attributed to the amorphization of brivaracetam within the polymer matrix, which increases the free energy and wettability of the drug, thereby improving dissolution behavior. Increasing pectin concentration tended to form a denser film matrix that slightly retarded drug release, whereas higher PEG 400 as plasticizer improved film flexibility and facilitated faster penetration of dissolution medium, thereby enhancing drug diffusion and release [31, 32]. The optimized formulation F2 shows the highest % of drug release ($98.94 \pm 4.6\%$) in 10 min. These findings confirm that pectin acts as a superior film-former and helps in drug release. These formulations show better % drug release compared to the formulation prepared by T. Rekhabei *et al.*, 2025, which had a % drug release of 95.61 ± 0.12 in 10 min [17].

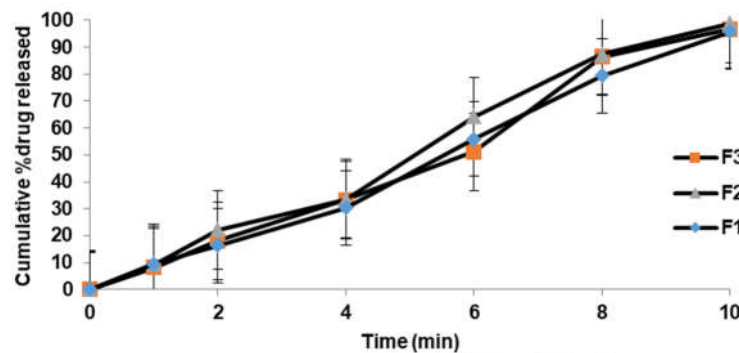


Fig. 8: *In vitro* drug release profiles of brivaracetam FDFs F1 to F3 (*n=6)

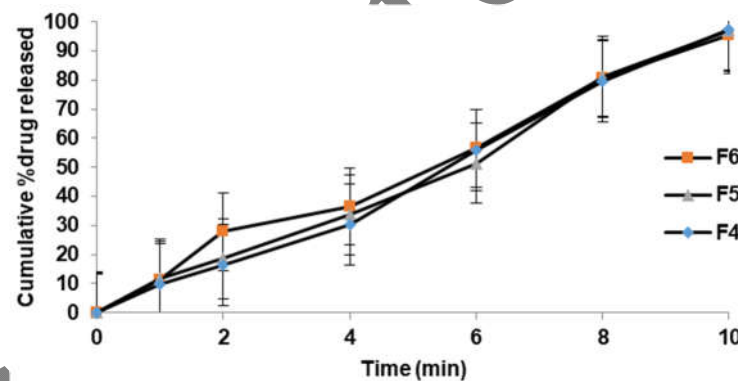


Fig. 9: *In vitro* drug release profiles of brivaracetam FDFs F4 to F6 (*n=6)

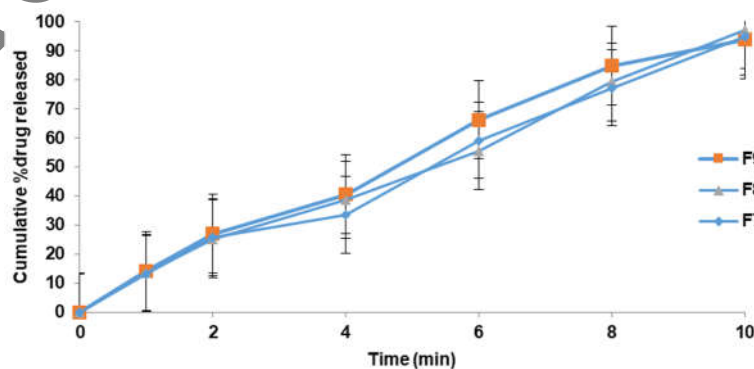


Fig. 10: *In vitro* drug release profiles of brivaracetam FDFs F7 to F8 (*n=6)

Nine FDF formulations from the 3² factorial design underwent DT (Y1) and TS (Y2) evaluation. Design-Expert® software fit data to quadratic polynomial models, assessing R², SD, and predicted residual sum of squares. Coded independent variables (A, B) generated equations predicting responses across levels.

Regression equation of the fitted quadratic model

$$DT(Y1) = -36.00 + 7.83A + 0.83B + 1.25AB + 0.50A^2 - 0.50B^2$$

$$\% TS (Y2) = +2.16 + 0.29A + 0.073B + 0.023AB - 0.033A^2 + 0.067B^2$$

Effect of independent variables on DT(Y1)

The response surface and contour plots show the effect of pectin (A) and PEG 400 (B) on disintegration time (DT). The plots and the polynomial equation indicate that DT increases with increasing pectin concentration, due to the formation of a thicker and more compact polymer matrix. ANOVA for the quadratic model demonstrated that the model was statistically significant, as shown in table 6 with an F-value of 11.16 and a corresponding p-value of 0.0374 (p<0.05), R² value (0.9490) indicating that the selected model adequately represents the relationship between the independent variables and the response. Three-dimensional response surface plots along with their corresponding two-dimensional contour plots illustrating the effects on DT are presented in fig. 11.

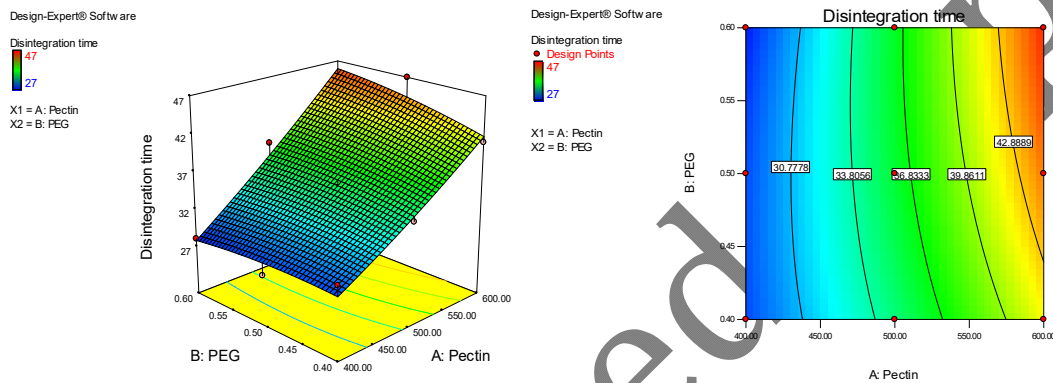


Fig. 11: Response surface and the corresponding 2D contour plots of DT

Table 6: ANOVA of the quadratic response surface model showing the effect of pectin and PEG 400 on DT

Source	Sum of SQUARES	df	Mean square	F-value	p-value	Prob>F
Model	379.58	5	75.92	11.16	0.0374	significant
A-Pectin	368.17	1	368.17	54.1	0.0052	
B-PEG	4.17	1	4.17	0.61	0.491	
AB	6.25	1	6.25	0.92	0.4086	
A ²	0.5	1	0.5	0.073	0.8039	
B ²	0.5	1	0.5	0.073	0.8039	
Residual	20.42	3	6.81			
Cor Total	400	8				

Effect of independent variables on TS(Y2)

Pectin concentration has a significant positive effect on the TS of FDFs. As the concentration of pectin increases, TS also increases, indicated by the curvilinear nature of the contour plots. The regression model exhibited a high F-value of 26.99 and a p-value of 0.0107 (p<0.05), confirming its statistical significance. The R² (0.9420) confirms the model's reliability. The ANOVA results of the resin shown in table 7. The three-dimensional response surface plots and corresponding two-dimensional contour plots for TS are presented in fig. 12.

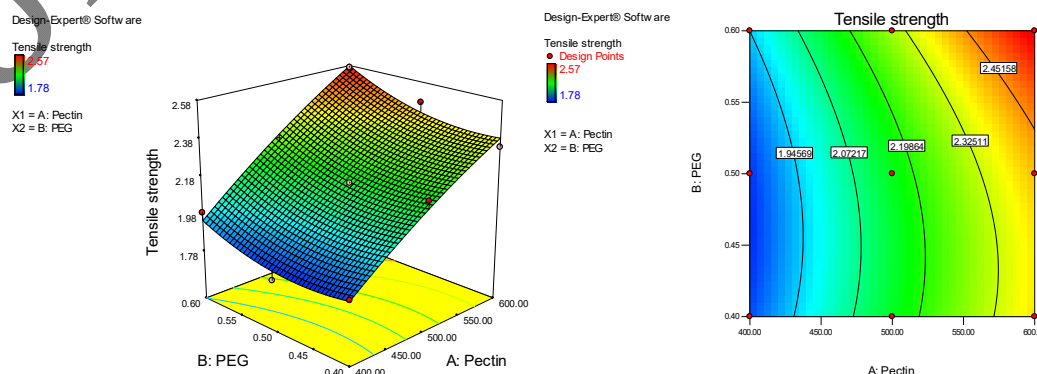


Fig. 12: Response surface and the corresponding 2D contour plots of TS

Table 7: ANOVA of the quadratic response surface model showing the effect of pectin and PEG 400 on TS

Source	Sum of squares	df	Mean square	F-value	p-value	Prob>F
Model	0.56	5	0.11	26.99	0.0107	significant
A-Pectin	0.52	1	0.52	124.04	0.0016	
B-PEG	0.032	1	0.032	7.75	0.0687	
AB	2.03E-03	1	2.03E-03	0.49	0.5357	
A2	2.22E-03	1	2.22E-03	0.53	0.5179	
B2	8.89E-03	1	8.89E-03	2.14	0.2401	
Residual	0.012	3	4.16E-03			
Cor Total	0.57	8				

Overlay plot

The overlay plot identifies the design space where all responses meet the desired criteria. The yellow region represents the optimal zone, while the grey area indicates non-compliant formulations. The optimized formulation (A=563.56 mg, B=0.41 ml) achieved disintegration time (39 ± 1 s) and tensile strength (2.30 ± 0.12 N/mm²) within acceptable limits. The interpretation of the overlay plot shown in fig. 13.

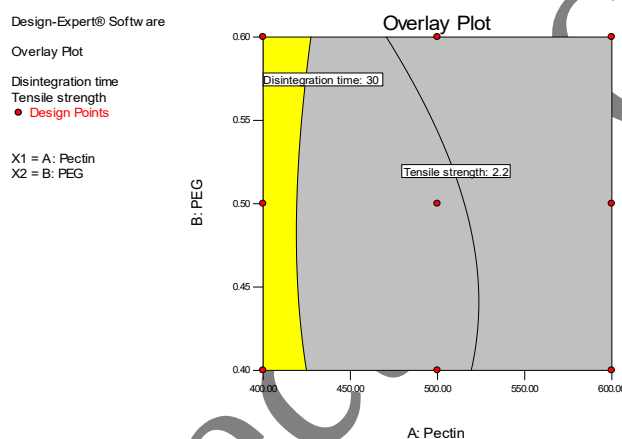


Fig. 13: Overlay plot of the optimized design space for brivaracetam FDFs, on DT, TS and %DD10, with the highlighted region indicating the optimum formulation zone

Stability studies

The stability of brivaracetam fast-dissolving films (FDFs) was evaluated in this study. Accelerated stability testing was conducted over a period of three months under conditions of 40 ± 2 °C and $75\pm 5\%$ relative humidity. TS, DT, drug content, and *in vitro* dissolution after 10 min were assessed at initial (0 d), 1 mo, and 3 mo intervals. The outcomes of the stability study are summarized in table 9. The TS and DT remained essentially unchanged, while drug content and *in vitro* dissolution showed only minimal variations. Statistical evaluation using a two-tailed Student's t-test comparing the initial and three mo values revealed no statistically significant differences ($p>0.05$) for all evaluated parameters. These findings confirm that the optimized brivaracetam FDFs remain stable under accelerated storage conditions.

Table 9: Accelerated stability study of optimized brivaracetam FDF formulation stored at 40 ± 2 °C/ $75\pm 5\%$ RH

Time point	Visual appearance	TS (N/mm ²)	DT (s)	Drug content (%)	%DD10
Initial	Transparent	1.78 ± 0.12	27 ± 2	97.06 ± 1.7	98.94 ± 4.6
1 mo	Transparent	1.76 ± 0.15	27 ± 2	95.09 ± 1.9	98.46 ± 2.3
2 mo	Transparent	1.77 ± 0.26	27 ± 1	98.64 ± 2.3	97.96 ± 3.7
3 mo	Transparent	1.78 ± 0.17	27 ± 2	97.81 ± 2.1	98.12 ± 3.4

Results are given as mean \pm SD, n=3. TS: Tensile strength; DT: Disintegration time; %DD10: Percentage drug dissolved in 10 min. Stability samples were stored under accelerated conditions (40 ± 2 °C/ $75\pm 5\%$ RH) as per ICH Q1A(R2). Statistical analysis was performed using paired Student's t-test comparing initial and 3 mo values, and no statistically significant difference was observed ($p>0.05$ for all parameters).

Validation and optimization

The statistical regression equation proposed by 3² was used for optimizing the brivaracetam FDFs. Based on the developed polynomial models, numerical optimization was performed using the desirability function approach to identify the optimal formulation conditions that satisfy the desired criteria of rapid disintegration, high drug release, and adequate mechanical strength. The responses were examined, and a single checkpoint formulation (VO) was prepared to verify the accuracy of the model. Table 10 displays the experimental and projected response values for the

validation batch. The validated batch contained pectin 563.56 and PEG 400 0.41 ml, showing 30 ± 1 sec DT, 2.30 ± 0.12 TS and $98.56 \pm 1.03\%$ of drug release after 10 min. The experimentally obtained responses showed good agreement with the predicted values, confirming the reliability of the optimization model.

Table 10: Validation batch of independent variables and their dependent responses

Independent variables		Dependent variables	
Pectin(A)	PEG(B)	DT (sec) (Y1)	TS(N/mm ²) (Y2)
563.56	0.41	30 ± 1	2.30 ± 0.12

Results are given as mean \pm SD, n=3

CONCLUSION

Brivaracetam FDFs were successfully formulated and optimized using a 3² factorial experimental design to evaluate the influence of pectin (A) and PEG 400 (B) on key formulation attributes. Among the tested formulations, the batch containing 400 mg of pectin and 0.5 ml of PEG 400 (F2) was identified as the optimized formulation through multi-response desirability analysis. The optimized film showed a drug content uniformity of $97.06 \pm 1.7\%$, DT of around 27 ± 2 sec, and %DD10 $98.94 \pm 4.6\%$, suggesting it is appropriate for rapid drug delivery of FDFs. The 3² factorial design effectively elucidated the influence of formulation variables on TS and DT. Stability studies demonstrated that the optimized formulation retained stability under accelerated storage conditions. The developed formulation offers a patient-friendly dosage form that may improve compliance, particularly in pediatric and geriatric populations experiencing difficulty in swallowing conventional tablets. The rapid disintegration and efficient drug release profile suggest its potential for faster onset of therapeutic action in epilepsy management.

ACKNOWLEDGEMENT

The author would like to express sincere gratitude to GITAM School of Pharmacy, Visakhapatnam, for their valuable support and assistance throughout this research work.

FUNDING

There is no funding to report.

AI STATEMENT

The authors declare that no generative AI tools were used for literature review, data analysis, image processing, and manuscript drafting.

AUTHORS CONTRIBUTIONS

Swetha's method selection, compilation of data, and writing the original draft. Dr. B. Janaki Devi supervised and edited the manuscript.

CONFLICT OF INTERESTS

The authors declare that there is no conflict of interest.

REFERENCES

- Anusha K, Rada SK. Oral disintegrating tablets: best approach for faster therapeutic action of poorly soluble drugs. *Egypt Pharm J*. 2021;20(2):105-14. doi: [10.4103/epj.epj_63_20](https://doi.org/10.4103/epj.epj_63_20).
- Velpula K. Preparation and evaluation of metronidazole matrix tablets for colon targeting. *WJPR*. 2017;2242-56. doi: [10.20959/wjpr20178-9122](https://doi.org/10.20959/wjpr20178-9122).
- Nishant DP, Bobade NN, Wankhade VP, Atram SC, Pande SD, Anuradha KS et al. Oral fast dissolving film: a review. *Asian J Pharm Res Dev*. 2025;13(2):148-56. doi: [10.22270/ajpr.v13i2.1553](https://doi.org/10.22270/ajpr.v13i2.1553).
- Badekar R, Bodke V, Tekade BW, Phalak SD. An overview on oral thin films—methodology, characterization and current approach. *Int J Pharm Pharm Sci*. 2024;16(4):1-10. doi: [10.22159/ijpps.2024v16i4.50386](https://doi.org/10.22159/ijpps.2024v16i4.50386).
- Račić A, Gatarić B, Topić Vučenović V, Stojmenovski A. Polysaccharide-based drug delivery systems in pediatrics: addressing age-specific challenges and therapeutic applications. *Polysaccharides*. 2025;6(4):108. doi: [10.3390/polysaccharides6040108](https://doi.org/10.3390/polysaccharides6040108).
- Narang B, Barve K, Wairkar S. Thermosensitive, mucoadhesive Brivaracetam nasal gel: a promising strategy for targeted relief of epilepsy. *Naunyn Schmiedeberg's Arch Pharmacol*. 2025;398(10):14301-13. doi: [10.1007/s00210-025-04172-1](https://doi.org/10.1007/s00210-025-04172-1), PMID 40285836.
- Rada SK, Kusuma A. Acute and sub-acute toxicity studies of starch hyaluronate in Wistar rats. *Trop J Nat Prod Res*. 2023;7(5):2965-8.
- Patel M, Desai T. A review on fast-dissolving oral film. *Asian J Pharm Clin Res*. 2023;16(10):100-5.
- Shah A, Patel K. Development and evaluation of therapeutically beneficial fast dissolving tablet containing herbal extracts: a quality by design approach. *Indian J Sci Technol*. 2025;18(9):682-95. doi: [10.17485/IJST/v18i9.3480](https://doi.org/10.17485/IJST/v18i9.3480).
- Phanapithakkun S, Yusakul G, Sitthisak C, Plyduang T. Development of tablet formulations containing genistein solid dispersion optimized using Box-Behnken design for enhanced solubility. *J Appl Pharm Sci*. 2025;15(4):053-64. doi: [10.7324/JAPS.2025.222224](https://doi.org/10.7324/JAPS.2025.222224).
- Kusuma A, Santosh Kumar R. Optimization of fast-dissolving tablets of carvedilol using 2³ factorial design. *Int J Appl Pharm*. 2024;16(1):98-107. doi: [10.22159/ijap.2024v16i1.49535](https://doi.org/10.22159/ijap.2024v16i1.49535).
- Mishra AS, Dutta G, Sugumaran A. Efficient fabrication and assessment of telmisartan fast-dissolving films using solvent casting approach. *Indian J Pharm Educ Res*. 2025;59(2s):s464-72. doi: [10.5530/ijper.20254097](https://doi.org/10.5530/ijper.20254097).
- Devi MG, R SK. Design, optimization and evaluation of ranolazine fast-dissolving films employing mango kernel starch as a new natural superdisintegrant. *Int J Appl Pharm*. 2024;16(6):271-81. doi: [10.22159/ijap.2024v16i6.51506](https://doi.org/10.22159/ijap.2024v16i6.51506).
- Kardile DP, Awate PB, Bhagat VC, Bhusari AC, Narote NA, Shete RV. Design, In-Vitro Characterization and Optimization of Fast Dissolving Sublingual Film containing Aripiprazole. *Res J Pharm Technol*. 2024;17(8):3725-9. doi: [10.52711/0974-360X.2024.00579](https://doi.org/10.52711/0974-360X.2024.00579).
- Angelevski S, Slaveska-Spirevska I, Lazarevska-Todevska E, Bakovska-Stoimenova T, Glavaš-Dodov M, Simonoska-Crcarevska M et al. Usporedna studija o proceni rizika elementarnih nečistoća u Montelukast tabletama za žvakanje i filmom obloženim tabletama. *Arh Farm*. 2023;73(1):74-87. doi: [10.5937/arhfarm73-41263](https://doi.org/10.5937/arhfarm73-41263).
- Anusha K, Venu K. Formulation and characterization of sustained release matrix tablets of verapamil hydrochloride using synthetic, semi-synthetic, and natural polymer. *World J Pharm Pharm Sci*. 2019;8(5):1633-44.

17. Rekhabai T, Kumar SK. Design and statistical optimization of muskmelon pectin-based telmisartan oral fast dissolving films through quality by design. *Int J Appl Pharm.* 2025;17(6):423-35. doi: [10.22159/ijap.2025v17i6.54850](https://doi.org/10.22159/ijap.2025v17i6.54850).
18. Moonesan M, Ganji F, Soroushnia A, Bagheri F. Fast-dissolving oral films containing dextromethorphan/phenylephrine for sinusitis treatment: formulation, characterization and optimization. *Prog Biomater.* 2022;11(3):243-52. doi: [10.1007/s40204-022-00191-w](https://doi.org/10.1007/s40204-022-00191-w), PMID 35796868.
19. Demchuk MB, Melnyk YY, Malanchyk NV, Groshovyi TA, Skorokhoda VY. Research the influence of excipients on the technological properties of captopril fast dissolving films. *Farm Zh.* 2022;2:61-72.
20. Sengar A, Yadav S, Niranjan SK. Formulation and evaluation of mouth-dissolving films of propranolol hydrochloride. *World J Pharm Res.* 2024 Jun 21;13(16):850-61.
21. Kamble RR, Magdum SS, Shah RR, Wadekar PP. Formulation and evaluation of ticagrelor nanosuspension loaded fast dissolving sublingual films. *Scopus Indexed.* 2025;18(3):8065-79. doi: [10.37285/ijpsn.2025.18.3.6](https://doi.org/10.37285/ijpsn.2025.18.3.6).
22. Ravulapati A, Achanti S, Kunderu RS, Lakshmi Kollipara NV, Shaik A. Innovative formulation and evaluation of sumatriptan fast dissolving tablets through 3² factorial design. *Curr Trends Biotechnol Pharm.* 2025;19(2s):52-60. doi: [10.5530/ctbp.2025.2s.5](https://doi.org/10.5530/ctbp.2025.2s.5).
23. Thummala UK, Maddi EG, Avula PR. Optimization of fast-dissolving tablets of Ledipasvirsofosbuvir inclusion complexes by design of experiments. *Indian J Pharm Educ Res.* 2023;57(1):33-44. doi: [10.5530/001954641530](https://doi.org/10.5530/001954641530).
24. Preis M, Knop K, Breitzkreutz J. Mechanical strength test for orodispersible and buccal films. *Int J Pharm.* 2014;461(1-2):22-9. doi: [10.1016/j.ijpharm.2013.11.033](https://doi.org/10.1016/j.ijpharm.2013.11.033), PMID 24291075.
25. Maheshwari S, Singh A, Varshney AP, Sharma A. Advancing oral drug delivery: the science of fast dissolving tablets (FDTs). *Intell Pharm.* 2024;2(4):580-7. doi: [10.1016/j.iph.2024.01.011](https://doi.org/10.1016/j.iph.2024.01.011).
26. Aulton ME, Taylor K. *Aulton's pharmaceuticals: the design and manufacture of medicines.* 5th ed. London: Elsevier; 2018. p. 56-64.
27. Mondal A, Ray P, Sen K, Dhara S, Ray SS, Kundu Sen S. Green-engineered domperidone oral fast dissolving film using *Artocarpus heterophyllus* fruit pulp biopolymer: physicochemical and biopharmaceutical characterization. *India. J Environ Manag.* 2026;398:407.
28. Maitra S, Das SK, Sen P, Mukherjee M, Sinha D, Roy T. Formulation optimization and *in vivo* evaluation of lorazepam mouth-dissolving films for rapid therapeutic onset in Swiss albino rats. *J Exp Zool India.* 2025;29(1):729-40. doi: [10.51470/jez.2026.29.1.729](https://doi.org/10.51470/jez.2026.29.1.729).
29. Costa BS, Pires CT, Chambi HN, Schmidt FL. Pectin orally disintegrating films containing jambolan juice (*Syzygium cumini*) and ginger: functional properties. *Ind Crops Prod.* 2025;226:120590. doi: [10.1016/j.indcrop.2025.120590](https://doi.org/10.1016/j.indcrop.2025.120590).
30. Godge RK, Khatal A, Mankar S, Vikhe K, Dighe S. Formulation and optimization of zopiclone co-crystal based fast-dissolving oral films for insomnia management. *BioNanoScience.* 2026;16(1):20. doi: [10.1007/s12668-025-02261-2](https://doi.org/10.1007/s12668-025-02261-2).
31. Dixit RP, Puthli SP. Oral strip technology: overview and future potential. *J Control Release.* 2009;139(2):94-107. doi: [10.1016/j.jconrel.2009.06.014](https://doi.org/10.1016/j.jconrel.2009.06.014), PMID 19559740.
32. Hancock BC, Parks M. What is the true solubility advantage for amorphous pharmaceuticals? *Pharm Res.* 2000;17(4):397-404. doi: [10.1023/A:1007516718048](https://doi.org/10.1023/A:1007516718048), PMID 10870982.